Analytical Biochemistry **292,** 171–177 (2001)
doi:10.1006/abio.2001.5084, available online at http://www.idealibrary.com on IDEAL®

In Vitro Assembly of Novel Cholera Toxin-like Complexes

Safet O. Hatic II,* Jameson A. McCann,†,[1] and William D. Picking*,[2]
**Department of Molecular Biosciences, University of Kansas, Lawrence, Kansas 66045; and †Department of Biology, Saint Louis University, St. Louis, Missouri 63103*

Received October 19, 2000; published online April 27, 2001

Cholera toxin (CT) is responsible for the major pathological features of cholera, but in addition to its cytotoxic properties, CT is a potent mucosal adjuvant when coadministered with antigens at mucosal sites. Discovery of CT adjuvanticity has prompted the generation of CT chimeras with reduced toxicity and improved efficiency for antigen presentation at mucosal sites. To date, chimeric forms of CT have been produced in bacterial strains by coexpressing the CT B subunit and a chimeric form of the CT A subunit consisting of a target protein antigen fused with the A2 polypeptide of CT. In this study, a chimeric protein consisting of green fluorescent protein (GFP) fused with polypeptide A2 was generated to investigate the feasibility of assembling CT holotoxin-like complexes *in vitro.* The assembly of such holotoxin-like complexes would expand the variety of antigenic compounds that could be incorporated into CT-based vaccines. In this study, GFP–A2/CTB complexes could be generated *in vitro* using a stepwise denaturation-renaturation process. These findings suggest that it is possible to generate novel mucosal vaccines consisting of macromolecules that are chemically coupled to polypeptide A2 and reconstituted into CT-like complexes *in vitro.* © 2001 Academic Press

The overt symptoms of cholera include abdominal cramps, fatigue, and profuse "rice-water" stools that result from the action of cholera toxin (CT)[3] secreted by *Vibrio cholerae* (1). CT is composed of five identical B protomers which associate with a 240-amino-acid A subunit that is proteolytically cleaved after residue 192 to give an N-terminal CTA1 protein linked by a disulfide bond to a C-terminal CTA2 polypeptide. CTA2 fits within the central pore of the B subunit pentamer (CTB) to tether CTA1 to the holotoxin (Fig. 1). CTB binds monosialoganglioside GM_1 (GM_1) on intestinal epithelial cells (1) to trigger endocytic uptake, transcytosis, and processing within the endosomal compartments of target cells (2, 3). Endosomal processing leads to reduction of the disulfide bridge linking CTA1 to CTA2 so that the former can be translocated into the target cell cytoplasm (4, 5). CTA1 then catalyzes ADP-ribosylation of $G_{s\alpha}$, a GTP-binding protein that is triggered to constitutively up-regulate adenylate cyclase (6). The resulting increase in cAMP leads to an osmotic imbalance and the efflux of water into the intestinal lumen (7).

In addition to being cytotoxic, CT is a powerful mucosal adjuvant that enhances the secretory (sIgA) immune response when coadministered with target antigens at mucosal sites (8). CT adjuvanticity may result from its adhesion to mucosal epithelial cells, its membrane-permeabilizing effects on cells, and/or its ability to stimulate the uptake of antigens at mucosal sites (8, 9). The generation of fusion proteins possessing novel proteins linked to the N-terminus of CTA2 has provided a potential strategy for generating CT-based mucosal vaccines having high efficacy (10, 11). Until recently, the only method described for obtaining such CT holotoxin-like complexes has been to coexpress *ctxb* and a *cta2*-fusion gene in a bacterial system for *in vivo* complex assembly (11). Preparation of the complex then requires purification of the CT-like molecule from the periplasm of the bacterial strain used for expression because these complexes are not transported across the bacterial outer membrane (11).

In this study, we generated a novel fusion protein consisting of green fluorescent protein (GFP) and CTA2 to explore the *in vitro* assembly of CT holotoxin-like complexes. This procedure is anticipated to allow the

[1] Present address: Department of Cellular and Molecular Physiology, Pennsylvania State College of Medicine, Hershey, PA 17033.

[2] To whom correspondence should be addressed. Fax: (785)864-5294. E-mail: picking@eagle.cc.ukans.edu.

[3] Abbreviations used: CT, cholera toxin; GFP, green fluorescent protein; EDC, 1-ethyl-3-(dimethylaminopropyl) carbodiimide; sulfo-NHS, *N*-hydroxysulfosuccinimide; GM_1, monosialoganglioside; IPTG, isopropyl thio-β-D-galactoside.

0003-2697/01 $35.00
Copyright © 2001 by Academic Press
All rights of reproduction in any form reserved.

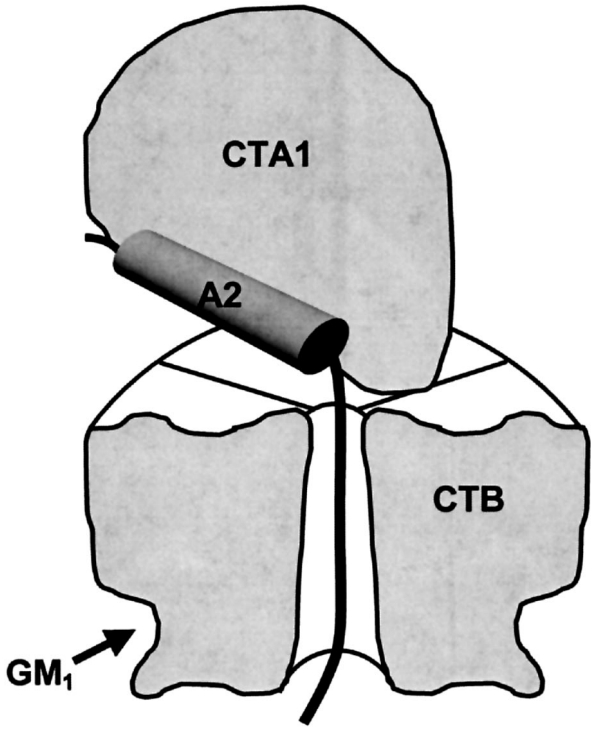

FIG. 1. A structural schematic of CT. This diagram shows a schematic representation of the general structure of the CT holotoxin. The exposed α-helix of polypeptide CTA2 fits within a groove on the lower surface of CTA1 and the two remain attached by a disulfide bridge involving the N-terminus of CTA2 and the C-terminus of CTA1. The C-terminus of CTA2 then resides (probably with helical structure) within a hydrophilic pore that extends through the center of the CTB pentamer (shown here as a cutaway to expose the central pore). CTB possess five GM_1 binding sites (indicated by the arrow). The very C-terminus of CTA2 is exposed beneath the CTB pentamer and possesses a KDEL sequence that targets CT for endosomal processing following endocytic uptake of toxin bound to a target cell surface.

preparation of CT-like molecules from individually purified protein components and should provide the basis for preparing complexes containing nonprotein antigenic components. In the latter case, it may be possible to chemically couple macromolecules to CT polypeptide A2 so that the resulting protein conjugate can be reconstituted with CTB *in vitro* to form a new class of CT-based mucosal vaccines.

MATERIALS AND METHODS

Materials. CT and CTB were from List Biologicals (Campbell, CA) and R. A. Finkelstein (University of Missouri, Columbia, MO). 1-Ethyl-3-(dimethylaminopropyl) carbodiimide (EDC) and *N*-hydroxysulfosuccinimide (sulfo-NHS) were from Pierce Chemicals (Rockford, IL). Monosialoganglioside GM_1 (GM_1), nickel sulfate, imidazole, and *p*-nitrophenyl phosphate were from Sigma Chemicals (St. Louis, MO); isopropyl thio-β-D-galactoside (IPTG), acetone, and methanol were from Fisher Scientific (St. Louis, MO); and affinity chromatography reagents were from Novagen (Madison, WI). Anti-GFP antibodies were from Clontech (Palo Alto, CA), anti-CTA antibodies were from Chemicon (Temecula, CA), and secondary antibodies were from Kirkegaard & Perry Labs (Gaithersburg, MD).

Plasmid construction. pMGJ60, containing *ctxAB* (11), was provided by R. K. Holmes (University of Colorado Health Sciences Center, Denver, CO) and the *cta2* coding region was copied by PCR and inserted into pET15b (Novagen) to give pJAMa2 (Fig. 2). *cta2* was then excised and placed into pET32 LIC to give pA2L. The *gfp* coding sequence was amplified by PCR and inserted into pA2L to give pJAMLga2, which was used to express a fusion protein consisting of thioredoxin (Trx), His_6, GFP and CTA2 (Fig. 2).

Protein preparation. Recombinant GFP-A2 was made from pJAMLga2 in *Escherichia coli* BL21(DE3) grown at 37°C in LB broth with 50 μg/ml ampicillin. GFP-A2 synthesis was induced with 1 mM IPTG for 12 h and the cells were collected by centrifugation. Cell pellets were resuspended in 20 mM Tris–HCl (pH 7.9), 0.5 M NaCl, and 5 mM imidazole and sonicated. The cell lysate was clarified by centrifugation at 20,000*g* and affinity chromatography was performed as previously described (12) using a nickel chelation resin. After being washed, bound protein was eluted with 20 mM Tris–HCl (pH 7.9), 0.5 M NaCl, and 1 M imidazole. Purified GFP-A2 possessed a Trx-His_6 leader that was removed by incubation with enterokinase, which specifically cleaved the fusion protein at the N-terminus of GFP. We previously used the Trx tag to enhance the solubility of recombinant bacterial proteins (13) and the presence of Trx at the N-terminus of the His_6 sequence appeared to enhance site-specific cleavage of the leader sequence from GFP-A2 (data not shown). Unprocessed GFP-A2 and cleaved leader were separated by passing the sample over a mini-nickel chela-

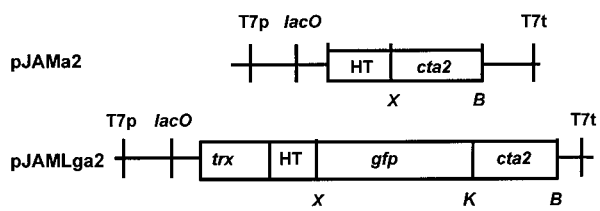

FIG. 2. Recombinant gene constructs. pJAMa2 encodes a His_6-containing leader sequence (HT) attached to CTA2. pJAMLga2 encodes a Trx–His tag (HT)–GFP–CTA2 fusion protein. The product of this gene can be cleaved with enterokinase to give GFP-A2. T7p is the T7 promoter, T7t is the T7 terminator and *lacO* is the *lac* operator. The locations of restriction sites for *Xho*I (X), *Kpn*I (K), and *Bam*HI (B) are also shown.

tion column, which removed the Trx–His_6 leader peptide. Final protein concentrations were determined by a BCA protein assay (Sigma Chemicals).

Reconstitution of CT holotoxin-like complexes. CT, CTB, and GFP-A2 were passed over Sephadex G25 equilibrated with water to remove the majority of the buffer. Protein samples were acid denatured for 20 min at 23°C at pH 2.3 by adding 1/10th vol 0.5 M citric acid. The solution was then neutralized with 0.12 vol 2 M Tris (pH 8.5) and the proteins were allowed to renature for at least 1 h.

Fluorescence measurements. Steady-state fluorescence spectroscopy of GFP-A2 was carried out on a Spex (Edison, NJ) FluoroMax spectrofluorometer (12). GFP-A2 was excited at 470 nm with emission scanned from 490 to 590 nm at 1 nm intervals with 0.1 s/wavelength increment. A peak of fluorescence with an emission maximum of 510 nm indicated that GFP-A2 was in an active conformation. A Beacon 2000 fluorescence polarization system (Panvera, Madison, WI) with a 480-nm bandpass excitation filter and a 530-nm bandpass emission filter was used to detect incorporation of active GFP-A2 into complexes with CTB. Polarization provides a measure of the average angular displacement of a fluorophore during its excited state lifetime. The rate of fluorophore depolarization is directly affected by its rotational diffusion rate, which is inversely related to its size. Because of the relationship between molecular volume and diffusion rate, polarization provides a sensitive measure of the changes in molecular volume that occur when a fluorescent species is incorporated into a macromolecular complex (14).

Cross-linking of proteins in reconstituted CT-like complexes. Protein cross-linking was used to monitor the formation of CTB/GFP-A2 complexes. EDC was added to a concentration of 10 mM in protein samples containing 10 mM sulfo-NHS. After 30 min, the samples were boiled in SDS buffer and the size of the resulting products determined by SDS–PAGE.

Ganglioside GM_1 (GM_1) ELISA. A GM_1-ELISA procedure was used to test the GM_1-binding activity of reconstituted complexes (15). Microtiter wells were coated with 0.1 μg GM_1 in 20 mM phosphate (pH 7.4), 150 mM NaCl (PBS). Open sites were blocked with 0.5% casein and diluted samples were then added to the wells for 1 h followed by washing with PBS. Primary antibodies were added for 1 h after which an alkaline phosphatase-conjugated secondary antibody was added (with extensive washing after each step). The chromogenic substrate *p*-nitrophenyl phosphate was then added at 1 mg/ml and the absorbance at 405 nm was measured after 30 min.

RESULTS

Denaturation and reactivation of GFP-A2 and CTB. GFP-A2 was produced in *E. coli* BL21(DE3) and the recombinant protein was purified to concentrations exceeding 6 mg/ml. The purified recombinant GFP-A2 was then treated with enterokinase to remove the Trx–His_6 region. Following protease treatment, the GFP-A2 moiety was typically present at concentrations of at least 2.5 mg/ml (in the same volume as the original sample), indicating that nearly 100% of the original protein was correctly processed since enterokinase is expected to remove about half of the mass of the original recombinant protein.

It has been shown that CTB and GFP can be denatured and refolded back into their active conformations (16, 17). Fluorescence spectroscopy was used to show that the GFP-A2 fusion protein is also denatured by low pH, and is readily refolded into an active conformation by neutralization of the sample. In Fig. 3A, the emission of GFP-A2 in water is shown using an excitation wavelength of 470 nm. When the pH is lowered to 3.0 or less, GFP-A2 fluorescence is eliminated due to unfolding of the protein (17); however, when the pH is neutralized, more than 80% of the original GFP-A2 fluorescence is recovered, indicating that the protein has been restored to its active conformation (Fig. 3A). To show that CTB is reconstituted into an active conformation following acid treatment, GM_1-binding was monitored. When CTB is denatured by low pH and then renatured, it regains more than 70% of its original GM_1-binding capacity based on a GM_1-ELISA assay employing antibodies against CT (Fig. 3B). Nearly 100% of the GM_1-binding capacity appears to be restored to CTB following stepwise denaturation and renaturation when ganglioside binding is monitored using the blue shift seen in the tryptophan fluorescence that is known to occur when CTB associates with GM_1 (data not shown) (18). These data indicate that both GFP-A2 and CTB refold into active conformations following exposure to the denaturation-renaturation conditions used here.

Formation of complexes containing GFP-A2 and CTB. To show that GFP-A2 can be assembled into complexes with CTB *in vitro*, the proteins were mixed and subjected to the same denaturation-renaturation process described above. The renatured proteins were then chemically cross-linked and the products analyzed by SDS–PAGE to determine the size of the cross-linked products. As shown in Fig. 4, the addition of EDC to a mixture of CTB and GFP-A2 following denaturation–renaturation results in the generation of a high-molecular-mass product with concomitant disappearance of bands representing pentameric CTB and monomeric GFP-A2. In contrast, the addition of cross-linking agent to the proteins that have been mixed but

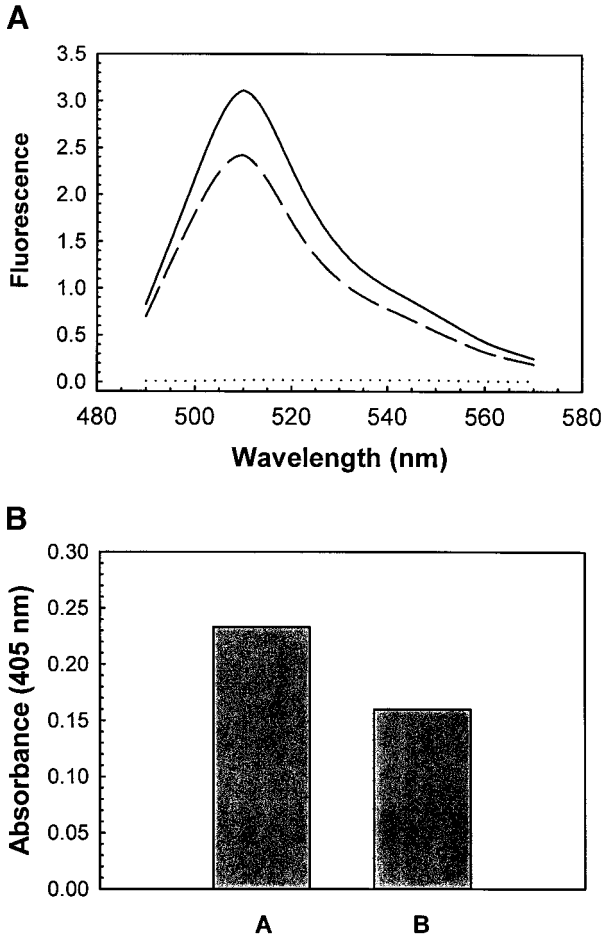

FIG. 3. GFP-A2 and CTB are renatured into active conformations. (A) The fluorescence spectrum of GFP-CTA2 at 23°C in water (solid line); following acidification with citric acid (dotted line); and following neutralization with Tris (dashed line) is shown using an excitation of 470 nm. The data shown are representative of three independent trials. (B) A GM_1 ELISA was used to determine the efficiency of reconstituting CTB into an active conformation following the treatments described in A. Based on absorbance at 405 nm, CTB regains more than 70% of its original activity under the conditions used. After denaturation and renaturation, the sample was diluted 1:100 with PBS and 10 μl was used for the GM_1 ELISA with anti-CT antibodies. Bar A is the ELISA result for CTB prior to denaturation and bar B is the result for the same amount of processed CTB. The data shown are the average of triplicate measurements with an error of less than 10%.

not subjected to the denaturation-renaturation process gives rise to CTB and GFP-A2 species that are approximately equivalent in size to the original CTB pentamer and GFP-A2 monomer (Fig. 4). These data indicate that complexes composed of CTB and GFP-A2 must be processed by denaturation and renaturation to form complexes *in vitro*.

GFP-A2/CTB complexes regain function after assembly. The CTB/GFP-A2 complex was anticipated to be on the order of 90 kDa; however, the complex observed after cross-linking appears to be much larger than expected (greater than 150 kDa). Because GFP-A2 fluorescence is recovered following denaturation-renaturation (Fig. 3), it seems unlikely that irreversible denaturation and nonspecific aggregation of the GFP-containing complex has occurred. Moreover, different forms of GFP have been described as forming dimers in solution (19) which could give rise to the high-molecular-weight form of GFP-A2/CTB seen by cross-linking analysis. To eliminate the possibility that inactive protein aggregates of CTB with GFP-A2 are formed as a result of the denaturation-renaturation process, it was important to show that the reconstituted complexes contain both active GFP-A2 and CTB.

Because of the native fluorescence of GFP-A2, fluorescence polarization was used to demonstrate its incorporation into complexes with CTB. Table 1 illustrates the polarization and intensity of GFP-A2 in the presence of a sixfold excess of CTB prior to denaturation, after denaturation, and following renaturation. This series of treatments should be sufficient to allow the assembly of GFP-A2/CTB complexes, which should give rise to an increase in the fluorescence polarization of GFP-A2 (Table 1). A potential difficulty in this experiment is that the starting polarization for GFP-A2 is relatively high because of the rigidity with which the chromophore of the active site is held at the interior of the large β-barrel structure of GFP (19). Despite this, reconstitution with CTB causes an observable increase

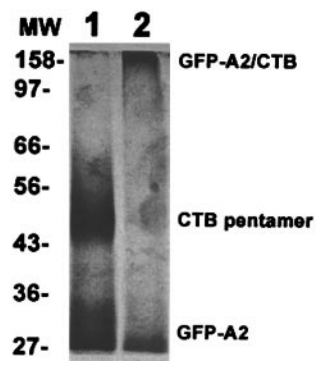

FIG. 4. Cross-linking analysis of GFP-A2/CTB complexes. SDS–PAGE with Coomassie blue staining was used to analyze complex formation by GFP-A2 and CTB after cross-linking with EDC. In lane 1, CTB and GFP-A2 were mixed but not processed by denaturation/renaturation prior to the addition of cross-linking agent. In lane 2, GFP-CTA2 and CTB were mixed, denatured, and then renatured, prior to the addition of cross-linking agent. The approximate positions of GFP-A2, the CTB pentamer, and the reconstituted GFP-A2/CTB complex are indicated. After cross-linking, the CTB pentamer and GFP-A2 migrate somewhat diffusely because the heterogeneity of intramolecular cross-links introduced into these proteins by EDC only allow the proteins to partially unfold (to varying degrees) in the presence of SDS. This causes the proteins to possess varying degrees of overall density, which leads them to migrate over a range of apparent molecular weights as measured by SDS–PAGE (giving rise to the observed diffuse bands).

TABLE 1

Fluorescence Polarization of GFP-A2 Increases Following Incorporation into Complexes with CTB

	Conditions	mP	Fluorescence intensity
A	CTB/GFP-A2 in water	349.3	1.00
B	A + 20 μl 0.5 M citric acid	299.1[a]	≤0.01[a]
C	B + 26 μl 2 M Tris (pH 8.5)	401.7	0.70

Note. Fluorescence polarization (millipolarization units or mP) was measured at 23°C on a Beacon 2000 fluorescence polarization system. The fluorescence intensity values shown are relative to the CTB/GFP-A2 mixture prior to denaturation.

[a] The results shown are representative data from three different experiments. Denaturation of GFP-A2 at low pH eliminates its fluorescence and prevents obtaining a reliable polarization value.

in GFP fluorescence polarization. The magnitude of this increase in GFP polarization (about 15%) is significant when it is considered that polarization has lower and upper limits of 0 and 500 mP and the rigid solution structure of GFP alone causes its polarization value to be 350 mP prior to complex formation. Moreover, CTA2 possesses an elongated structure that is expected to behave as a flexible tether rather than one that tightly fixes GFP to the surface of the CTB pentamer, thereby limiting the extent to which CTB association could cause GFP-A2 polarization to increase. In contrast, when the same experiment is carried out in the absence of CTB, GFP-A2 regains its original polarization value and more than 75% of its original total fluorescence (data not shown). These data suggest that the GFP-A2 incorporated into protein complexes with CTB is active since inactivated GFP-A2 would be nonfluorescent and incapable of contributing to the observed increase in polarization. From the data in Fig. 4 and Table 1, it is clear that GFP-A2/CTB complexes possessing active GFP-A2 can be assembled *in vitro*.

To determine if the CTB associated with GFP-A2 is also in an active conformation, a GM_1 ELISA using primary antibodies against GFP was used to monitor the ganglioside-binding capacity of the GFP-A2-containing protein complexes. As shown in Fig. 5, GFP-A2/CTB complexes specifically bind to GM_1 coated onto the surface of 96-well plates. As with the cross-linking experiments described above, the formation of this active complex requires that the CTB/GFP-A2 mixture be subjected to stepwise denaturation and renaturation (Fig. 5). Furthermore, the ability for the complex to bind to the 96-well plates is dependent upon the presence of GM_1.

To determine the efficiency for the formation of active GFP-A2/GFP complexes, a concentration curve for GFP-A2 coated onto microtiter plate wells was used to determine what percentage of the theoretical yield of this protein was being assembled into CT holotoxin-like complexes (data not shown). Using the same conditions as those used for the experiment described in Fig. 5, excess GFP-A2 was added to CTB and the mixture was reconstituted by acidification followed by neutralization. When the maximum amount of GFP-A2 that should be able to assemble with the amount of CTB pentamer used in the experiment was calculated and compared to the actual amount of GFP-A2 that associated with active CTB, assembly was found to occur with about 20% efficiency.

DISCUSSION

When fully denatured, cholera toxin separates into five CTB monomers and a single CTA protein (1). Following separation into its constituent monomers, CT can be reassembled *in vitro* in a process that requires complex interactions between its A subunit and its five B monomers (20). Using recombinant proteins possessing CTA2 fused at their carboxyl termini, it has been shown that CT holotoxin-like complexes can be formed in bacteria, indicating that CTA2 is sufficient for directing the formation of hybrid CT complexes (11). Such hybrids represent a novel approach for creating a new generation of specific mucosal vaccines (8, 10, 11). Here we provide the first description of the *in vitro* assembly of a chimeric form of CT using native CTB and GFP that has been genetically fused with the polypeptide CTA2 (GFP-A2). The assembly of this

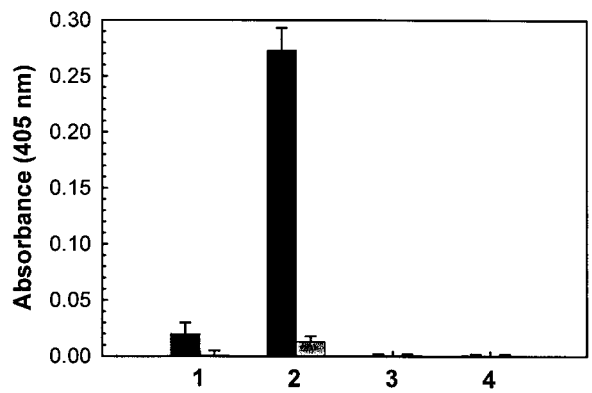

FIG. 5. Binding of the CTB/GFP-A2 complex to GM_1. A GM_1 ELISA using primary antibodies against GFP was used to show that GFP-A2 was incorporated into complexes capable of binding ganglioside GM_1. The black bars indicate the absorbance (405 nm) for wells coated with ganglioside GM_1 and the gray bars show the absorbance for the same samples in wells lacking GM_1. In experimental set 1, 8 μg CTB and 25 μg GFP-A2 were mixed but not subjected to a denaturation-renaturation step. In 2, the same amount of CTB and GFP-A2 was mixed and subjected to denaturation/renaturation. In 3, 25 μg GFP-A2 was processed in the absence of CTB and in 4, 8 μg CTB was processed in the absence of GFP-A2. In each case, an aliquot (1/5th volume) was removed for analysis using commercial anti-GFP antibodies. The data are average values (±SD) from a single experiment performed in triplicate and are representative of the results obtained in three separate experiments.

novel holotoxin-like complex requires that the components be mixed, denatured to unfold the proteins (using low pH here), and then renatured to allow the simultaneous folding of CTB and GFP-A2.

We previously described the formation of a holotoxin-like molecule consisting of CTB and only the A2 portion of CTA (12); however, the work presented here extends those studies by demonstrating that a large, relatively rigid structure such as that of GFP can be fused to the N-terminus of CTA2 without compromising the ability for CTA2 to direct holotoxin assembly *in vitro.* More importantly, these *in vitro* assembled complexes still retain their ability to bind ganglioside GM_1, an activity that is essential for CTB biological function. Furthermore, *in vitro* assembly of the CT-like complexes described here does not lead to inactivation of the protein species fused with CTA2. It should be noted that the denaturation/renaturation conditions used to assemble CT-like molecules when CTA2 is fused with proteins other than GFP may need to be adjusted when the aim is to restore those proteins to an active conformation. However, when the ultimate goal is to generate an effective immunogen, it may not be essential to have an active form of the protein incorporated into the CT holotoxin-like complex. Therefore, as long as CTA2 is available for association with the central pore of CTB during the denaturation/renaturation process, nearly any protein should be capable of being incorporated *in vitro* into a CT-based vaccine.

Novel forms of CT represent valuable tools for generating mucosal immune responses against important microbial pathogens (8–11). The ability to generate such complexes *in vitro* shows that CT-based mucosal vaccines consisting of components that could not be assembled in *E. coli* cloning strains can now be generated. For example, *in vitro* assembly of CTB with CTA2-containing molecules could be carried out when the CTA2 fusion protein needs to be synthesized in a eukaryotic expression system to generate glycosylated forms of the antigen. Alternatively, such a system would provide a means for conjugating nonprotein structures to CTA2 (possibly via the single cysteine residue near its N-terminus) prior to *in vitro* assembly with CTB. In such cases, an understanding of the principles involved in the *in vitro* assembly of CT holotoxin-like molecules would be extremely useful.

It is not yet possible to tell whether the formation of complexes composed of target antigens linked with CTA2 and incorporated into CT holotoxin-like complexes will be uniformly useful for generating mucosal vaccines. Data from other laboratories in which CT-like chimeras were synthesized in bacterial systems appear to provide a promising outlook (10). The primary goal of this study was to determine the feasibility for creating CT-like protein complexes *in vitro,* which could lead to the generation of CT-like chimeras possessing antigens that could not be genetically coupled to CTA2. While it is not within the immediate scope of this communication to test the efficacy of such mucosal vaccines, it is anticipated that future work along these lines will greatly expand the repertoire of mechanisms available for combating pathogens that initiate infection at mucosal sites.

ACKNOWLEDGMENT

We acknowledge technical assistance and helpful discussions with Wendy L. Picking (Department of Molecular Biosciences, University of Kansas).

REFERENCES

1. Spangler, B. D. (1992) Structure and function of cholera toxin and the related *Escherichia coli* heat-labile enterotoxin. *Microbiol. Rev.* **56,** 622–647.
2. Lencer, W. I., Moe, S., Rufo, P. A., and Madara, J. L. (1995) Transcytosis of cholera toxin subunits across model human intestinal epithelia. *Proc. Natl. Acad. Sci. USA* **92,** 10094–10098.
3. Orlandi, P. A., Curran, P. K., and Fishman, P. H. (1993) Brefeldin A blocks the response of cultured cells to cholera toxin. *J. Biol. Chem.* **268,** 12010–12016.
4. Mekalanos, J. J., Collier, R. J., and Romig, W. R. (1979) Enzymic activity of cholera toxin. II. Relationships to proteolytic processing, disulfide bond reduction, and subunit composition. *J. Biol. Chem.* **254,** 5855–5861.
5. Moss, J., Tsai, S. C., and Vaughan, M. (1994) Activation of cholera toxin by ADP-ribosylation factors. *Methods Enzymol.* **235,** 640–647.
6. Galloway, T. S., and van Heyningen, S. (1987) Binding of NAD^+ by cholera toxin. *Biochem. J.* **244,** 225–230.
7. Peterson, W. J., and Ochoa, L. G. (1989) Role of prostaglandins and cAMP in the secretory effects of cholera toxin. *Science* **245,** 857–859.
8. Holmgren, J., Lycke, N., and Czerkinsky, C. (1993) Cholera toxin and cholera toxin B subunit as oral-mucosal adjuvant and antigen vector systems. *Vaccine* **11,** 1179–1184.
9. Lycke, N., Karlsson, U., Sjolander, A., and Magnusson, K. E. (1991) The adjuvant action of cholera toxin is associated with an increased intestinal permeability for lumenal antigens. *Scand. J. Immunol.* **33,** 691–700.
10. Hajishengallis, G., Hollingshead, S. K., Koga, T., and Russell, M. W. (1995) Mucosal immunization with a bacterial protein antigen genetically coupled to cholera toxin A2/B subunits. *J. Immunol.* **154,** 4322–4332.
11. Jobling, M. G., and Holmes, R. K. (1992) Fusion proteins containing the A2 domain of cholera toxin assemble with B polypeptides of cholera toxin to form immunoreactive and functional holotoxin-like chimeras. *Infect. Immun.* **60,** 4915–4924.
12. McCann, J. A., and Picking, W. D. (1997) Purification of recombinant cholera toxin polypeptide A2 and reconstitution with the cholera toxin B subunit. *Protein Peptide Lett.* **4,** 39–46.
13. Picking, W. L., Mertz, J. A., Marquart, M. E., and Picking, W. D. (1996) Cloning, expression, and affinity purification of recombinant *Shigella flexneri* invasion plasmid antigens IpaB and IpaC. *Protein Express. Purif.* **8,** 401–408.
14. Lakowicz, J. R. (1983) Principles of Fluorescence Spectroscopy, Plenum, New York.
15. Liljeqvist, S., Stahl, S., Andreoni, C., Binz, H., Uhlen, M., and Murby, M. (1997) Fusions to the cholera toxin B subunit: influ-

ence on pentamerization and GM1 binding. *J. Immunol. Methods* **210,** 125–135

16. De Wolf, M. J. S., and Dierick, W. S. H. (1994) Regeneration of active receptor recognition domains on the B subunit of cholera toxin by formation of hybrids from chemically inactivated derivatives. *Biochim. Biophys. Acta* **1223,** 285–295.
17. Ward, W. W., and Bokman, S. H. (1982) Reversible denaturation of *Aquorea* green-fluorescent protein: Physical separation and characterization of the renatured protein. *Biochemistry* **21,** 4535–4540.
18. De Wolf, M. J. S., Fridkin, M., and Kohn, L. D. (1981) Tryptophan residues of cholera toxin and its A and B protomers. *J. Biol. Chem.* **256,** 5489–5496.
19. Tsien, R. Y. (1998) The green fluorescent protein. *Annu. Rev. Biochem.* **67,** 509–544.
20. Hardy, S. J. S., Holmgren, J., Johansson, S., Sanchez, J., and Hirst, T. R. (1988) Coordinated assembly of multisubunit proteins: oligomerization of bacterial enterotoxins *in vivo* and *in vitro*. *Proc. Natl. Acad. Sci. USA* **85,** 7109–7113.